Enhanced Kerr Nonlinearity via Atomic Coherence in a Three-Level Atomic System

Hai Wang,* David Goorskey, and Min Xiao†

Department of Physics, University of Arkansas, Fayetteville, Arkansas 72701

(Received 23 March 2001; published 26 July 2001)

We measure the Kerr-nonlinear index of refraction of a three-level Λ-type atomic system inside an optical ring cavity. The Kerr nonlinearity is modified and greatly enhanced near atomic resonant conditions for both probe and coupling beams. The Kerr nonlinear coefficient n_2 changes sign when the coupling beam frequency detuning switches sign, which can lead to interesting applications in optical devices such as all-optical switches.

DOI: 10.1103/PhysRevLett.87.073601 PACS numbers: 42.50.Gy, 32.80.Qk, 42.65.–k

One of the intriguing aspects of atomic coherence in multilevel atomic systems is its ability to enhance the efficiencies of nonlinear optical processes. The atomic coherence induced by coupling and probe laser beams can reduce the resonant absorption of the probe beam through electromagnetically induced transparency (EIT) [1–3] and enhance the resonant nonlinear interaction strength in multilevel atomic systems. Furthermore, the steep dispersion slope [4] in such EIT systems can significantly reduce the group velocity of probe pulses [4,5] and, therefore, greatly increase the effective interaction length of a probe pulse with the atomic medium, which makes it possible to perform nonlinear optical processes with very low light intensities [6–8]. In the past few years, several experimental demonstrations of enhancing nonlinear optical processes (such as optical harmonic generation [9], frequency conversion [10], and near-degenerate four-wave mixing [11,12]) were reported in multilevel atomic systems. Also, EIT-induced beam focusing [13] and elimination of optical self-focusing by atomic coherence [14] were observed in three-level atomic systems. Although these enhanced nonlinear processes can be experimentally demonstrated by observing the generated nonlinear optical signals, it is still a difficult task to directly measure the nonlinear coefficients associated with these nonlinear processes because of the existence of the linear absorption and dispersion effects. A large Kerr-nonlinear index of refraction is particularly interesting in multilevel atomic systems, since it can be used for many interesting applications, such as cross-phase modulation for optical shutters, self-phase modulation for generating optical solitons, four-wave mixing processes for frequency conversion, and entangled states for quantum information processing [6–8]. Direct measurement of the Kerr-nonlinear coefficient will greatly help us to understand and to optimize the nonlinear optical processes in these multilevel atomic systems, to make direct comparison with theoretical predictions, and to find more practical applications of this Kerr-like nonlinearity.

In this Letter, we report an experimental demonstration of how this Kerr-nonlinear coefficient n_2 in a three-level atomic system can be directly measured by using an optical ring cavity through enhanced nonlinear phase shift and suppressed linear effects. We consider a typical three-level Λ-type ^{87}Rb atomic system, as used in Ref. [15], with $F = 1$ (state $|1\rangle$) and $F = 2$ (state $|3\rangle$) states of $5S_{1/2}$ as the two lower states and $F' = 2$ (state $|2\rangle$) of $5P_{1/2}$ as the upper state. The coupling laser beam (with frequency ω_c and Rabi frequency Ω_c) couples states $|3\rangle$ and $|2\rangle$ while the probe laser beam (with frequency ω_p and Rabi frequency Ω_p) interacts with states $|1\rangle$ and $|2\rangle$. The coupling frequency detuning is defined as $\Delta_c = \omega_c - \omega_{23}$ and the probe frequency detuning as $\Delta_p = \omega_p - \omega_{12}$. With a relatively strong coupling beam, e.g., $\Omega_c \gg \Omega_p$, most atoms will be optically pumped into the ground level $|1\rangle$. To calculate the nonlinear susceptibility for the probe beam, we keep the probe intensity to higher (third) order and derive the following expression for the susceptibility between states $|1\rangle$ and $|2\rangle$ as

$$\chi \approx \frac{iN|\mu_{21}|^2}{\hbar}\frac{1}{F}\left[1 - \frac{2\gamma_{31}}{2\gamma + \gamma_{21}} - \frac{|\Omega_p|^2}{(2\gamma + \gamma_{21})}\frac{F + F^*}{|F|^2}\right], \quad (1)$$

with $F \equiv \gamma - i\Delta_p + (|\Omega_c|^2/4)/[\gamma_{31} - i(\Delta_p - \Delta_c)]$. $\gamma \equiv (\gamma_{21} + \gamma_{23} + \gamma_{31})/2$; γ_{21} and γ_{23} are the spontaneous decay rates of the excited state $|2\rangle$ to the ground states $|1\rangle$ and $|3\rangle$, respectively; γ_{31} is the nonradiative decay rate between two ground states. N is the atomic density in the cell and μ_{21} is the dipole matrix element between states $|1\rangle$ and $|2\rangle$. The first term in Eq. (1) is the linear susceptibility as given in Ref. [3], the second term is the contribution to linear susceptibility from the higher-order density matrix element, and the third term is the third-order (or Kerr-like) nonlinearity due to the finite probe intensity as defined by $\chi \approx \chi^{(1)} + 3\chi^{(3)}|E_p|^2$ and is modified by atomic coherence. $E_p = -\Omega_p\hbar/\mu_{21}$ is the probe field amplitude. The Kerr nonlinear index of refraction n_2 is defined by

$$n_2 = \frac{12\pi^2}{n_0^2 c}\,\mathrm{Re}\chi^{(3)} = \mathrm{Re}\left[-\frac{i4\pi^2N|\mu_{21}|^4}{cn_0^2\hbar^3}\frac{1}{(2\gamma + \gamma_{21})}\frac{F + F^*}{F\cdot|F|^2}\right], \quad (2)$$

where n_0 is the linear index of refraction. For atoms in a vapor cell, one can take into account the higher-order

Doppler effects by integrating Eq. (2) over a Maxwellian velocity distribution, as described in Ref. [3] for the linear susceptibility. The first-order Doppler effect is eliminated by copropagating the coupling and probe beams through the atomic cell inside the optical ring cavity [3]. By examining Eq. (2), one can see that n_2 has peaks near resonance for both probe and coupling frequency detunings. If one neglects γ_{31} and residual Doppler effects, the peaks will appear at $\Delta_p \approx \pm\Omega_c/2$ for $\Delta_c = 0$ with $n_2 > 0$ for $\Delta_p = -\Omega_c/2$ and $n_2 < 0$ for $\Delta_p = +\Omega_c/2$. If one sets $\Delta_p = 0$ and tunes the coupling frequency, i.e., varies Δ_c, n_2 will behave in an opposite way since Δ_c acts similar to Δ_p in Eq. (2) except with an opposite sign. When Eq. (2) is integrated over velocity distribution, the above conditions will be modified, but the qualitative behaviors will remain.

When a nonlinear medium is placed inside an optical cavity, the intensity-dependent index of refraction will introduce a nonlinear phase shift $\Delta\Phi^{\mathrm{NL}}$ to the cavity resonant condition when the cavity length is scanned through its resonance. The cavity phase detuning is modified by the nonlinear phase shift as

$$\delta = \frac{2\pi[(n_0 - 1)L + L_c]}{\lambda} + \frac{2\pi L}{\lambda} n_2 I_p + \varphi_0 - 2\pi m, \tag{3}$$

where L is the length of medium; L_c is the cavity length; m is an integer; λ is the wavelength of the probe light; ϕ_0 is the phase offset of the cavity; I_p is the intracavity intensity of the probe beam. When the cavity length is scanned linearly with time and the nonlinear phase shift (proportional to $n_2 I_p$) is negligible, the cavity transmission profile is a simple Lorentzian shape. However, with the nonlinear phase shift, the cavity transmission profile becomes asymmetric and the degree of asymmetry is determined by n_2 [16].

Our experimental setup is shown in Fig. 1. Both the coupling (LD1) and the probe (LD2) lasers are single-mode diode lasers that are current and temperature stabilized. The frequencies of these two diode lasers are further stabilized by using optical feedback through servo-loop controlled mirrors. The linewidths of the coupling and probe lasers are both about 1.0 MHz. Parts (about 10%) of the probe and coupling beams are split by polarizing beam splitters PBS1 and PBS2 to a saturation absorption spectroscopy (SAS) setup to monitor the frequency detunings of the two lasers. The optical ring cavity is composed of three mirrors. The flat mirror M1 and the concave mirror M2 ($R = 10$ cm) have about 1% and 3% transmissions, respectively. The third cavity mirror (concave with $R = 10$ cm) is mounted on a piezoelectric transducer (PZT) with reflectivity larger than 99.5%. The finesse of the empty cavity is about 100 with a free spectral range of 822 MHz (cavity length is 37 cm). The rubidium vapor cell is 5 cm long with Brewster windows and is wrapped in μ metal and heated to 63 °C. The probe beam enters the

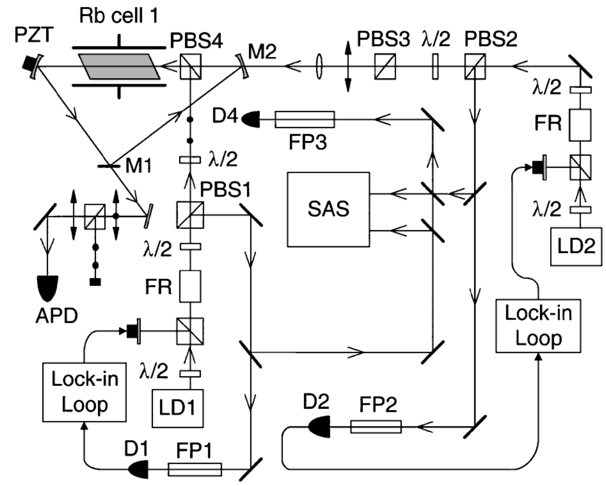

FIG. 1. Experimental setup. LD1 and LD2 are coupling and probe diode lasers, respectively; PBS1–PBS4 are polarizing cubic beam splitters; $\lambda/2$, half-wave plates: FR, Faraday rotators; FP1–FP3, Fabry-Perot cavities; D1–D4, detectors; SAS is the unit for saturation absorption spectroscopy; APD, avalanche photodiode detector.

cavity through mirror M2 and circulates inside the optical ring cavity. The coupling beam is introduced through the polarization beam splitter PBS4 with orthogonal polarization to the probe beam and is misaligned by a small angle (about two degrees) to avoid its circulation inside the optical cavity. The cavity is mode matched to the probe beam using a 15 cm focal length lens. The radii of the coupling and probe beams are estimated to be 700 μm and 80 μm, respectively. With the insertion losses of the PBS4 and reflections from the windows of the atomic cell, the cavity finesse (with rubidium atoms far off resonance) is degraded to about 50. The probe input intensity of the cavity is controlled by PBS3 and a half-wave plate. The frequencies of both the probe and coupling beams are controlled precisely by locking to Fabry-Perot cavities FP1 and FP2. The frequency detunings of the two beams are measured separately by another Fabry-Perot cavity (FP3).

We first tune and lock the coupling beam to the resonant frequency of the coupling transition ($5S_{1/2}, F = 2$—$5P_{1/2}, F' = 2$), e.g., $\Delta_c = 0$. Then, we tune and lock the probe beam to be on resonance with the probe transition ($5S_{1/2}, F = 1$—$5P_{1/2}, F' = 2$) or set it to be a few MHz above or below resonance. The injected coupling intensity into the atomic cell is about 20 mW, which corresponds to an average Rabi frequency of $\Omega_c = 2\pi \times 72$ MHz in the atomic cell. The peak intracavity intensity (with cavity on resonance) is estimated to be about 6 μW, which corresponds to a Rabi frequency of $\Omega_p = 2\pi \times 11$ MHz at the center of the cell. The length of the optical ring cavity is scanned by the PZT mounted on one of the cavity mirrors and the cavity transmission is measured by an avalanche photodiode (APD) detector. When the coupling beam is blocked (no EIT), the cavity transmission profile is basically symmetric as shown in Fig. 2a with $\Delta_p = 7$ MHz.

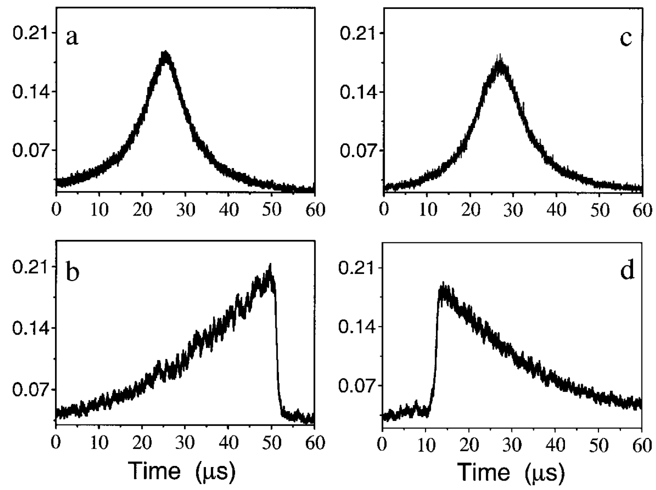

FIG. 2. Cavity transmission profiles for (a) $\Delta_p = 7$ MHz, $\Omega_c = 0$, and a FWHM linewidth of 20 MHz; (b) $\Delta_p = 7$ MHz, $\Delta_c = 0$, $\Omega_c = 2\pi \times 72$ MHz; (c) $\Delta_p = -7$ MHz, $\Omega_c = 0$, and a FWHM linewidth of 22 MHz; (d) $\Delta_p = -7$ MHz, $\Delta_c = 0$, $\Omega_c = 2\pi \times 72$ MHz.

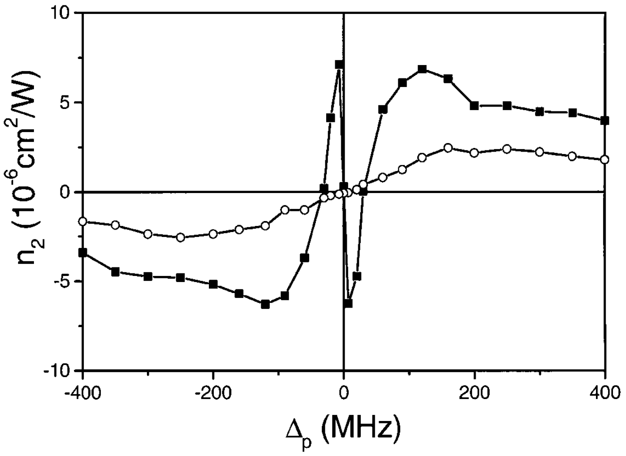

FIG. 3. Measured Kerr-nonlinear coefficient n_2 versus frequency detuning of probe beam with $\Delta_c = 0$ and $\Omega_c = 2\pi \times 72$ MHz. Solid squares are with coupling beam and open circles are without coupling beam.

With the coupling beam turned on (with EIT), the cavity transmission profile becomes asymmetric, as shown in Fig. 2b. The degree of asymmetry in the cavity transmission profile is a direct measure of the nonlinear phase shift, which is proportional to the Kerr-nonlinear index of refraction n_2. The direction of the asymmetry gives the sign of the nonlinear coefficient n_2. As the cavity length is scanned from shorter to longer, the intracavity intensity will take longer to reach the peak power if n_2 is negative (as in Fig. 2b), which can be seen in a simple relation $\delta = \frac{2\pi}{\tau}(t - t_0) + \frac{2\pi L}{\lambda} n_2 I_p$, as given by Eq. (3), where τ is the time period between two transmission peaks when the cavity length is scanned. When the intracavity intensity increases (as the phase detuning approaches zero), the nonlinear phase shift (proportional to the increased intensity I_p) will act against it since the second term has opposite sign from the first term. When n_2 is positive, the asymmetry in cavity transmission will behave in an opposite fashion, as shown in Fig. 2d, when the frequency of the probe beam is tuned to $\Delta_p = -7$ MHz. Figure 2c is measured when the coupling beam is blocked with $\Delta_p = -7$ MHz. The Kerr-nonlinear index of refraction n_2 can be directly obtained by [16]

$$n_2 = \frac{\lambda[(t_1 - t_r) - (t_r - t_2)]}{2\tau(I_r - I_\delta)L}, \tag{4}$$

where I_r is the peak intensity of the cavity transmission reached at time t_r; t_1 and t_2 are the values of scan time t when the intracavity intensity rises to and falls to the same intensity I_δ (which is about half of the peak intensity I_r), respectively. All the parameters in Eq. (4) can be measured in experimental curves such as the ones shown in Fig. 2.

Figure 3 plots the measured Kerr-nonlinear index of refraction n_2 for different probe beam detunings with coupling beam on resonance (solid squares) and without the coupling beam (open circles). When the probe frequency is tuned across the EIT-modified absorption profile, the intracavity intensity will also change. During experimental measurements for different probe detuning values, we keep the same intracavity peak intensity by altering the input power of the probe beam for the cavity. As one can see, near the probe resonant frequency, the Kerr-nonlinear index of refraction n_2 is greatly enhanced at the EIT condition and has sharp changes. This behavior is consistent (both in shape and in magnitude) with results from theoretical calculation using Eq. (2) with Doppler broadening included. The factor of about 2 difference in nonlinearity for probe frequency detunings outside ± 200 MHz is due to optically pumping the population from one ground state ($5S_{1/2}, F = 2$) to another ($5S_{1/2}, F = 1$). The large enhancement of more than 2 orders of magnitude in nonlinearity at near resonance ($\Delta_p \approx \pm 7$ MHz for given Ω_c) is quite significant. Actually, the positions of maximal nonlinear coefficient n_2 can be tuned away from the resonant frequency by increasing Ω_c as predicted by our theoretical calculation based on Eq. (2) with Doppler broadening.

Another interesting effect in this system is to fix the probe frequency on resonance and tune the coupling frequency. Figure 4 shows the measured Kerr-nonlinear index of refraction n_2 as a function of coupling detuning with $\Delta_p = 0$. Such behavior is also predicted by Eq. (2) since the roles of the coupling detuning and probe detuning are different only by sign. This effect can have an interesting application in switching the sign and amplitude of the nonlinearity of the probe beam by simply tuning the coupling frequency in a small range (a few MHz), which can be used for all-optical switching, beam profile controlling, and other nonlinear optical processes.

The measured n_2 (about 7.0×10^{-6} cm^2/W) is quite large compared to the achievable values in regular two-level atomic media. This enhancement is due to the atomic

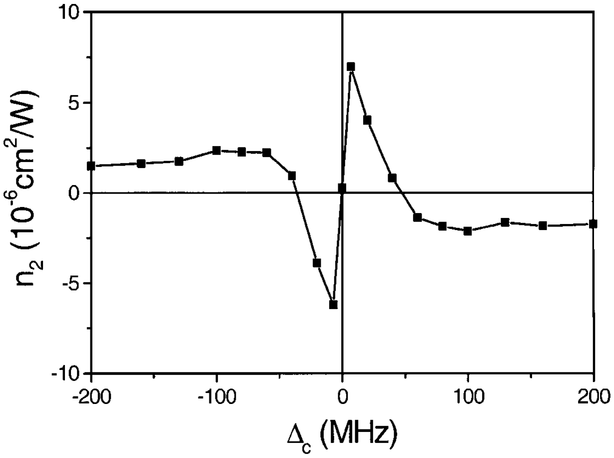

FIG. 4. Measured Kerr-nonlinear coefficient n_2 versus frequency detuning of the coupling beam with $\Delta_p = 0$ and $\Omega_c = 2\pi \times 72$ MHz.

coherence effect induced by the coupling beam as can be easily seen from Eq. (2). Several factors prevent us from making direct comparison between our theoretical calculations [Eq. (2) with integration over the velocity distribution] and the experimentally measured results (Figs. 3 and 4). For example, the transverse beam profiles of the laser beams and the nonuniformity of the laser intensities along the atomic cell are not considered in the theoretical treatment. Also, the poor cavity finesse due to cavity losses (atomic absorption, reflections from atomic cell windows, and cube polarizing beam splitter), cavity instability, and frequency stability of the diode lasers all contribute to the uncertainties in the experimental measurements. Despite all these problems, the calculated Kerr-nonlinear index of refraction n_2 from Eq. (2) with integration over the velocity distribution with realistic experimental parameters is consistent (both in shape and magnitude) with the experimentally measured n_2 values.

We would like to point out that the nonlinear index of refraction n_2 measured in our experiment is different from the nonlinear coefficient presented in Refs. [5,13], where the nonlinear term is proportional to $n_2' I_c$ (which relates to the slope of linear dispersion), not $n_2 I_p$ (which arises from nonlinear susceptibility $\chi^{(3)}$) as in the current work.

In summary, we have directly measured the Kerr-nonlinear index of refraction of a three-level EIT system by using an optical ring cavity. This technique eliminates contributions from the linear absorption and dispersion and can be used for measuring nonlinear behaviors of other atomic systems, such as proposed four-level systems [6,7]. The experimentally measured nonlinear enhancement is quite significant and is consistent with the calculated values with realistic experimental parameters. Such direct studies of the nonlinear coefficient will help us to understand, optimize, and eventually lead to a complete control of the nonlinear optical processes in such atomic systems. There are interesting applications (such as in all-optical switches and beam shaping) for the controllable nonlinearity (sign, magnitude, and maximal position in detuning) of the probe beam by simply changing the frequency and intensity of the coupling (or controlling) beam.

This work was supported in part by the National Science Foundation and the Office of Naval Research.

*On leave from the Institute of Opto-Electronics, Shanxi University, Shanxi, People's Republic of China.
†Email address: mxiao@mail.uark.edu

[1] S. E. Harris, Phys. Today **50**, No. 7, 36 (1997); E. Arimondo, in *Progress in Optics XXXV,* edited by E. Wolf (Elsevier, Amsterdam, 1996), p. 257.
[2] K. L. Boller, A. Imamoglu, and S. E. Harris, Phys. Rev. Lett. **66**, 2593 (1991); J. E. Field, K. H. Hahn, and S. E. Harris, Phys. Rev. Lett. **67**, 3062 (1991).
[3] J. Gea-Banacloche, Y. Li, S. Jin, and M. Xiao, Phys. Rev. A **51**, 576 (1995); Y. Li and M. Xiao, Phys. Rev. A **51**, R2703 (1995).
[4] M. Xiao, Y. Li, S. Jin, and J. Gea-Banacloche, Phys. Rev. Lett. **74**, 666 (1995).
[5] L. V. Hau, S. E. Harris, Z. Dutton, and C. H. Behroozi, Nature (London) **397**, 594 (1999); M. Kash *et al.,* Phys. Rev. Lett. **82**, 5229 (1999); D. Budker, D. F. Kimball, S. M. Rochester, and V. V. Yashchuk, Phys. Rev. Lett. **83**, 1767 (1999).
[6] S. E. Harris and L. Hau, Phys. Rev. Lett. **82**, 4611 (1999); S. E. Harris and Y. Yamamoto, Phys. Rev. Lett. **81**, 3611 (1998).
[7] A. Imamoglo, H. Schmodt, G. Woods, and M. Deutsch, Phys. Rev. Lett. **79**, 1467 (1997).
[8] M. D. Lukin, S. F. Yelin, and M. Fleischhauer, Phys. Rev. Lett. **84**, 4232 (2000); M. D. Lukin *et al., ibid.* **81**, 2675 (1998).
[9] K. Hakuta, L. Marmet, and B. P. Stoicheff, Phys. Rev. Lett. **66**, 596 (1991).
[10] A. J. Merriam *et al.,* Phys. Rev. Lett. **84**, 5308 (2000); M. Jain, H. Xia, G. Y. Yin, A. J. Merriam, and S. H. Harris, Phys. Rev. Lett. **77**, 4326 (1996).
[11] P. R. Hemmer *et al.,* Opt. Lett. **20**, 982 (1995).
[12] B. Lu, W. H. Burkett, and M. Xiao, Opt. Lett. **23**, 804 (1998); Y. Li and M. Xiao, Opt. Lett. **21**, 1064 (1996).
[13] R. R. Moseley *et al.,* Phys. Rev. Lett. **74**, 670 (1995).
[14] M. Jain, A. J. Merriam, A. J. Kasapi, G. Y. Yin, and S. E. Harris, Phys. Rev. Lett. **75**, 4385 (1995).
[15] H. Wang, D. J. Goorskey, W. H. Burkett, and M. Xiao, Opt. Lett. **25**, 1732 (2000).
[16] Z. Y. Ou, Opt. Commun. **124**, 430 (1996).